双椭球热源参数的敏感性分析及预测

李培麟，　陆　皓
（上海交通大学 材料科学与工程学院，上海　200240）

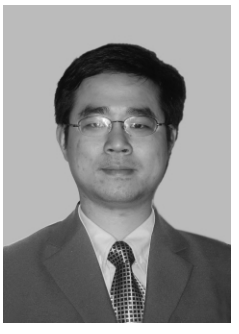

李培麟

摘　要：双椭球模型是在电弧冲击力较大的情况下常用的热源模型. 通过研究双椭球热源模型的参数对焊接熔宽、熔深的影响，获得双椭球热源模型的形状参数在埋弧焊中的敏感性. 并为了研究特定熔宽与熔深情况下对应的热源模型参数，采用多元回归分析，提出了敏感性分析的经验公式，获得了熔宽熔深与热源参数之间的关系. 通过回归获得的经验公式，可以在已有熔宽熔深试验结果的条件下获得对应的热源参数，简化热源模型的试算过程，提高了模拟的效率和精度.

关键词：埋弧焊；双椭球热源；敏感性；多元回归
中图分类号：TG402　　**文献标识码**：A　　**文章编号**：0253－360X(2011)11－0089－03

0　序　　言

埋弧焊作为一种高效率的焊接工艺，已经在压力容器、造船、桥梁、工程机械、核电设备等制造中成为了一个重要的焊接手段. 由于埋弧焊的熔敷效率和焊接速度较大，因此提高了埋弧焊的工作效率.

埋弧焊由于其焊接速度快、熔深大、电弧对熔池的冲击作用大，因此采用常用的高斯热源模型无法模拟埋弧焊的热源. 而双椭球热源模型由于加入了工件深度方向的参数，能够反映出热源在工件深度方向上的加热情况，因此双椭球热源模型成为在埋弧焊模拟中常用的热源模型[1]. 然而双椭球模型的参数选择会对模拟的结果产生相当大的影响，但具体参数的选取多根据经验而定. 由于参数较多，在尝试时通常需要花较多的时间，效率低下. Goldak 等人[2]曾经建议采用熔宽的一半作为双椭球模型的宽度参数，熔深作为双椭球模型的深度参数，前半椭球长度参数采用熔宽的一半，后半椭球长度参数采用熔宽的两倍. 然而这一假设通常是不准确的. 王煜等人[3]提出了通过解析法获得电子束焊接的双椭球参数，然而解析法是基于点状连续移动热源的解析方程，对于传热过程进行了一定程度的假设，在精度方面存在一定缺陷.

文中提出了双椭球热源参数对于埋弧焊的影响，为利用双椭球模型进行埋弧焊提供了参数选取的依据，并试图通过建立埋弧焊的双椭球热源参数变化对于熔宽及熔深影响的方程，使焊接模拟过程中减少对双椭球参数的试算次数. 对于特定的焊接熔宽及熔深结果，通过模拟计算可以直接获得焊接过程的温度场及应力等结果.

收稿日期：2010－09－16
基金项目：国家自然科学基金资助项目(50975176)

1　计算模型的设置

1.1　热源模型及几何模型

热源模型采用双椭球模型，其方程为

$$q_{\mathrm{f}}(x,y,z,t) = \frac{f_{\mathrm{f}}\eta UI6\sqrt{3}}{\pi\sqrt{\pi}a_{\mathrm{f}}bc}\cdot\exp\left(-3\left(\frac{x-vt}{a_{\mathrm{f}}}\right)^2-3\left(\frac{y}{b}\right)^2-3\left(\frac{z}{c}\right)^2\right) \tag{1}$$

$$q_{\mathrm{r}}(x,y,z,t) = \frac{f_{\mathrm{r}}\eta UI6\sqrt{3}}{\pi\sqrt{\pi}a_{\mathrm{r}}bc}\cdot\exp\left(-3\left(\frac{x-vt}{a_{\mathrm{r}}}\right)^2-3\left(\frac{y}{b}\right)^2-3\left(\frac{z}{c}\right)^2\right) \tag{2}$$

式中：$f_{\mathrm{f}}+f_{\mathrm{r}}=2$，为热源分布参数；$\eta$ 为热源效率；U 为电弧电压；I 为焊接电流；a_{f} 和 a_{r} 分别为前半椭球和后半椭球的长度参数；b 为椭球宽度参数；c 为椭球深度参数；v 为焊接速度；t 为时间.

计算采用平板工件. 长为 600 mm，半宽为 300 mm，厚为 22 mm，焊接所用电流与电压分别为 1 000 A，32 V，焊接速度为 16.67 mm/s. 对于平板对接问题，关于焊道中心的纵向截面为对称面，可以将模型简化为取一半宽度的对称简化模型. 由于焊道周围的温度梯度较大，远离焊接工作区域的温度梯度较小，因此在模型中将焊道附近的网格加以细化. 而

远离焊接工作区域的温度梯度较小,采用粗网格能减少计算时间. 粗细网格之间使用四面体网格进行过渡.

考虑到试板有坡口存在,因此对模型相应区域进行切割,制造出坡口的形状. 上坡口由于有焊丝填缝,对上坡口的区域内的单元加入生死单元技术,将第一根丝扫过的区域单元活化,而第一根丝尚未扫过的区域则设置为死单元. 由于坡口的存在,热源中心将会比后置丝的热源中心降低一些. 这里将热源中心降低至坡口底部. 在计算至 18 s 时模型和网格划分如图 1 所示.

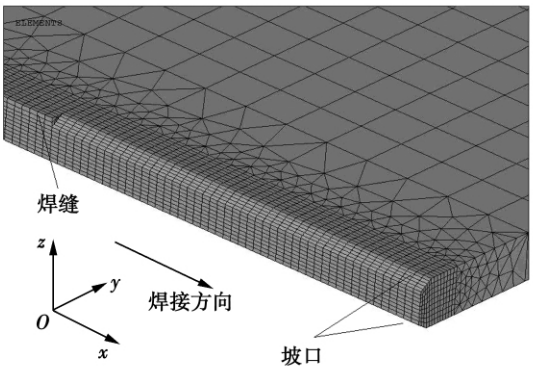

图 1 计算所用的几何模型和网格划分

Fig. 1 Geometry model and mesh generation

模型中以焊接方向为 x 轴正向,板的正法向为 z 轴正向,板的宽度方向为 y 轴,方向以右手螺旋法则确定. 原点设置在第一根丝的起点处.

考虑工件向环境的辐射散热条件,辐射换热的方程为

$$q_{\mathrm{R}} = A\varepsilon\sigma(T^4 - T_a^4) \tag{3}$$

式中: A 为辐射面的表面积; ε 为辐射黑度,这里定义 $\varepsilon = 0.8$; $\sigma = 5.67 \times 10^{-8}$ W/(m^4·K^4),为史蒂芬-玻尔兹曼常数; T 和 T_{a} 分别为辐射面与环境的绝对温度.

同时考虑了工件表面的对流换热为

$$q_{\mathrm{C}} = h(T - T_{\mathrm{a}}) \tag{4}$$

式中: h 为对流换热系数,在这里将其定义 $h = 3.0$ W/(m^2·K).

1.2 敏感性分析数学模型

在这个模型中,输入参数为双椭球参数 a_{f}, a_{r}, b, c 以及焊接速度 v,输出参数为熔宽 w 和熔深 p. 回归方程设计为[4]

$$\left.\begin{aligned} w(a_{\mathrm{f}},a_{\mathrm{r}},b,c,v) &= x_{1w}a_{\mathrm{f}}^{x_{2w}}a_{\mathrm{r}}^{x_{3w}}b^{x_{4w}}c^{x_{5w}}v^{x_{6w}} \\ p(a_{\mathrm{f}},a_{\mathrm{r}},b,c,v) &= x_{1p}a_{\mathrm{f}}^{x_{2p}}a_{\mathrm{r}}^{x_{3p}}b^{x_{4p}}c^{x_{5p}}v^{x_{6p}} \end{aligned}\right\} \tag{5}$$

式中: x_{iw}, x_{ip} ($i = 1,2,\cdots,6$) 分别为待定系数.

对式(5)求自然对数可获得

$$\left.\begin{aligned} \ln w &= \ln x_{1w} + x_{2w}\ln a_{\mathrm{f}} + x_{3w}\ln a_{\mathrm{r}} + x_{4w}\ln b + \\ &\quad x_{5w}\ln c + x_{6w}\ln v \\ \ln p &= \ln x_{1p} + x_{2p}\ln a_{\mathrm{f}} + x_{3p}\ln a_{\mathrm{r}} + x_{4p}\ln b + \\ &\quad x_{5p}\ln c + x_{6p}\ln v \end{aligned}\right\} \tag{6}$$

对于式(6),可以进行线性拟合,通过线性拟合获得待定参数 x_{iw} 和 x_{ip} 的最佳值.

2 计算结果及敏感性分析

2.1 对标准状况的试算

为计算热源参数的敏感性,首先必须获得某特定工艺下的热源参数. 在这里采用 $I = 1\,000$ A, $U = 32$ V 的焊接工艺作为标准状态. 通过对埋弧焊的实际焊缝情况的测量以及试算,获得了如表 1 所示的热源参数.

表 1 特定工艺条件下的埋弧焊热源参数

Table 1 Heat source parameter

前轴 a_{f}/mm	后轴 a_{r}/mm	宽度 b/mm	深度 c/mm
3.5	10.5	3.5	12.0

试算与试验获得的熔宽、熔深情况对比见表 2.

表 2 试算与试验结果对比

Table 2 Comparison between experiment and simulation

试验熔宽 w_{e}/mm	计算熔宽 w_{c}/mm	熔宽误差 e_w(%)	试验熔深 p_{e}/mm	计算熔深 p_{c}/mm	熔深误差 e_p(%)
15.88	16.42	3.40	14.03	14.14	0.78

试算结果与实际结果相当接近,此热源参数可以作为参数敏感性测试的标准值.

2.2 参数敏感性

对埋弧焊的双椭球参数 a_{f}, a_{r}, b, c 以及焊接速度 v 分别进行 0.8, 0.9, 1.1, 1.2 倍的调整,并进行数值模拟以获得对应的熔宽熔深结果. 然后代入式(6)进行线性拟合. 将获得的敏感性参数代入式(5),即

$$\left.\begin{aligned} w &= \frac{496.91}{a_{\mathrm{f}}^{0.0157}a_{\mathrm{r}}^{0.0233}b^{0.0083}c^{0.5411}v^{0.7113}} \\ p &= \frac{15.53c^{0.3113}}{a_{\mathrm{f}}^{0.0096}a_{\mathrm{r}}^{0.0108}b^{0.0527}v^{0.2730}} \end{aligned}\right\} \tag{7}$$

回归结果与计算结果对比见图 2. 两者最大误差小于 6%,可见回归结果能反映计算结果的规律.

从式(7)可见,随着热源参数及焊接速度的增大,熔宽减小. 然而 a_{f}, a_{r}, b 对于熔宽的影响非常

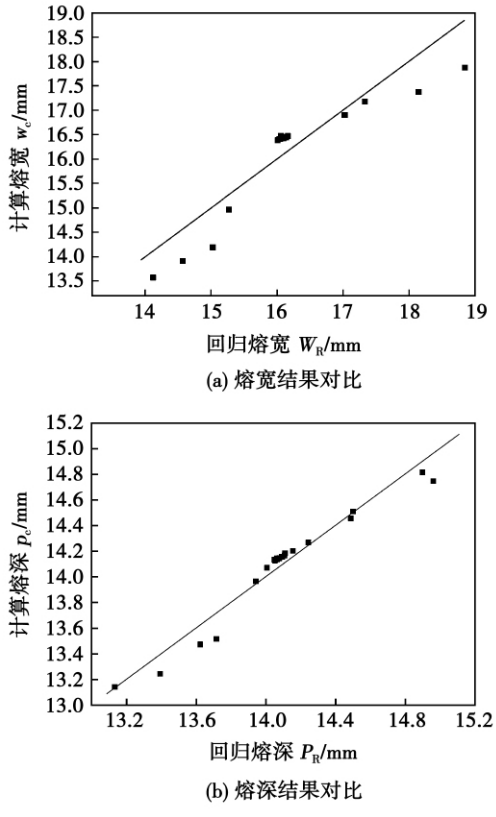

图 2　回归结果与计算结果对比

Fig. 2　Comparison of regression and calculation results

小,主要是深度参数 c 以及焊接速度 v 对熔宽的影响较大. 熔深受到 c 以及 v 的影响远大于 a_f,a_r,并且 b 对熔深的结果也有一定影响. 同时,随着 c 的增加,熔深也随之增加. 对熔宽熔深造成影响的参数主要为宽度 b、深度 c、焊接速度 v.

3　模型参数预测

3.1　参数预测的数学模型

对于式(6),由于未知量数目多于方程数目,因此方程为不定方程. 解决的方法主要有增加方程数目与减少自变量数目两种. 由于增加方程数目必须增加熔池形貌测点,增加了工作量,因此文中主要以减少自变量数目为目的.

对于热源参数的预测,w,p,v 为已知参数,a_f,a_r,b,c 为待定参数. 由于方程只有两个,因此自变量数目必须控制为 2. 考虑到对熔宽熔深造成影响的参数主要为宽度参数 b、深度参数 c、焊接速度 v,而长度参数 a_f 与 a_r 对焊接的影响较小,考虑到热源模型的形状,将 a_f 与 a_r 作 $a_f = b$,$a_r = 3b$ 的简化.

x_{iw} 及 x_{ip} 通过对式(6)的拟合已经获得. 将已知、未知参数分离可得

$$\begin{pmatrix} \ln w - x_{6w}\ln v - \ln x_{1w} - x_{3w}\ln 3 \\ \ln p - x_{6p}\ln v - \ln x_{1p} - x_{3w}\ln 3 \end{pmatrix} = \begin{pmatrix} x_{2w} + x_{3w} + x_{4w} & x_{5w} \\ x_{2p} + x_{3p} + x_{4p} & x_{5w} \end{pmatrix} (\ln b \quad \ln c)^{\mathrm{T}} \tag{8}$$

通过对矩阵求逆并将式(7)的结果代入后得

$$\begin{pmatrix} \ln b \\ \ln c \end{pmatrix} = \begin{pmatrix} -5.733\,9 & -9.965\,8 \\ -1.347\,1 & 0.870\,8 \end{pmatrix} \times \begin{pmatrix} \ln w + 0.711\,3\ln v - 6.182\,8 \\ \ln p + 0.273\,0\ln v - 2.730\,6 \end{pmatrix} \tag{9}$$

通过式(9)可以获得在特定熔宽熔深及焊接速度情况下所对应的热源参数.

3.2　参数预测的验证

为验证式(9)的经验公式,设计了如表 3 所示的实际焊接情况. 将表 3 的参数代入式(9),得到对应的热源参数见表 4. 模拟获得的熔池形貌结果及误差结果见表 5.

表 3　验证模型参数

Table 3　Verification of model parameters

	熔宽 w/mm	熔深 p/mm	焊接速度 v/(mm·s^{-1})
1	17.0	14.7	15.5
2	16.5	14.0	17.0
3	14.5	13.5	18.0

表 4　验证热源参数

Table 4　Verification heat source parameters

	前轴 a_f/mm	后轴 a_r/mm	宽度 b/mm	深度 c/mm
1	2.71	8.13	2.71	12.19
2	2.79	8.37	2.79	11.37
3	5.70	17.11	5.70	12.59

表 5　验证结果

Table 5　Verification results

	试验熔宽 w_e/mm	计算熔宽 w_c/mm	熔宽误差 e_w(%)	试验熔深 p_e/mm	计算熔深 p_c/mm	熔深误差 e_p(%)
1	17.0	16.95	−0.29	14.7	14.55	−1.02
2	16.5	16.47	−0.18	14.0	13.94	−0.43
3	14.5	14.07	−2.97	13.5	13.12	−2.81

从表 5 的分析可以看出,式(9)在对热源参数进行预测的方面有着较高的精度,误差在 3% 以内. 通过式(9)可以获得特定熔池形态以及焊接速度所对应的热源参数,从而通过数值模拟等手段可以获得焊接过程中的瞬态温度场、应力等较为精确的结果.

[下转第 95 页]

试件焊缝组织明显细化,抗拉强度和断后伸长率明显提高.

(2) 振幅对振动焊接的接头力学性能有明显影响,在振幅为 0.06 mm 时,焊接试件的抗拉强度和断后伸长率分别提高了 6% 和 37.8%.

(3) 随着振幅增大,使焊接参数发生扰动,焊接试件的力学性能没有继续提高,反而产生焊接缺陷影响焊接质量.

参考文献:

[1] 上田修三. 结构钢的焊接-低合金钢的性能及冶金学[M]. 荆洪阳, 译. 北京: 冶金工业出版社, 2004.

[2] 朱政强, 陈立功, 倪纯珍. 振动焊接工艺的研究现状及发展方向[J]. 焊接, 2003(5): 5-7.
Zhu Zhengqiang, Chen Ligong, Ni Chunzhen. Research state and developing direction of vibratory welding technology[J]. Welding & Joining, 2003(5): 5-7.

[3] Concharevich I F, Frolov K V, Rivin E I. Theory of vibratory technology[M]. New York: Hemisphere Publishing Corporation, 1990.

[4] 张国福, 宋天民, 尹成江, 等. 机械振动焊接对焊缝及热影响区金相组织的影响[J]. 焊接学报, 2001, 22(3): 85-87.
Zhang Guofu, Song Tianmin, Yin Chengjiang, *et al*. The effect of mechanical vibration welding on the microstructure of weld and HAZ[J]. Transactions of the China Welding Institution, 2001, 22(3): 85-87.

[5] 陈金涛, 宫照坤, 曲　牡, 等. 振动焊接对焊缝力学性能的影响[J]. 大连理工学报, 2001, 41(1): 35-37.
Chen Jintao, Gong Zhaokun, Qu Mu, *et al*. The effect of vibertion welding on mechanical performanceof weld[J]. Jouranl of Dalian Science and Engineering College, 2001, 41(1): 35-37.

[6] 张德芬, 陈孝文, 宋天民, 等. 机械振动提高焊接接头冲击吸收功[J]. 焊接学报, 2003, 24(5): 85-87.
Zhang Defen, Chen Xiaowen, Song Tianmin, *et al*. Studay of mechanical vibertion welding on impact energy[J]. Transactions of the Chian Welding Institution, 2003, 24(5): 85-87.

[7] 朱政强, 张　华, 陈立功, 等. 振动对焊缝金属动力力学性能的影响[J]. 中国机械工程, 2007, 18(7): 859-861.
Zhu Zhengqiang, Zhang Hua, Chen Ligong, *et al*. Influence of vibertion on the dynamic mechanics properties of weld metal[J]. Journal of Chinese of Mechanical Engineering, 2007, 18(7): 859-861.

[8] 崔忠圻. 金属学与热处理[M]. 北京: 机械工业出版社, 1995.

[9] Babu S S, David S A. Development of macro-and microstructures of carborn-manganese low alloy stell welds: inclusion formation[J]. Journal of Materials Science & Technology, 1995, 11(2): 186-189.

作者简介: 刘政军,男,1962 年出生,教授,博士研究生导师. 主要从事焊接冶金、特种焊接材料及表面强化方向的研究. 发表论文 90 余篇. Email: Liuzhengjun1962@163.com

[上接第 91 页]

4 结　　论

(1) 通过对不同热源参数的情况进行拟合,获得了双椭球热源模型参数对埋弧焊有限元计算的敏感性经验公式. 经模拟与回归结果对比,两者误差小于 6%.

(2) 对敏感性经验公式加以改进,获得了在特定熔池形状以及焊接速度条件下预测所对应的热源参数的经验公式. 对预测经验公式进行了实际验证,发现误差在 3% 以内,可以满足预测的需要.

(3) 在进行埋弧焊的有限元模拟时,对于不同工艺的焊接模拟,可以通过热源模型预测经验公式获得对应的热源参数,从而降低试算的工作量,简化计算的准备工作,提高计算精度.

参考文献:

[1] 莫春立, 钱百年, 国旭明, 等. 焊接热源计算模式的研究进展[J]. 焊接学报, 2001, 22(3): 93-96.
Mo Chunli, Qian Bainian, Guo Xuming, *et al*. The development of models about welding heat sources' calculation[J]. Transactions of the China Welding Institution, 2001, 22(3): 93-96.

[2] Goldak J, Chakravarti A, Bibby M. A new finite element model for welding heat sources[J]. Metallurgical Transactions, 1984, 15(2): 299-305.

[3] 王　煜, 赵海燕, 吴　甦, 等. 高能束焊接双椭球热源模型参数的确定[J]. 焊接学报, 2003, 24(2): 67-70.
Wang Yu, Zhao Haiyan, Wu Su, *et al*. Shape parameter determination of double ellipsoid heat source model in numerical simulation of high energy beam welding[J]. Transactions of the China Welding Institution, 2003, 24(2): 67-70.

[4] Karaoğlu S, Seçginb A. Sensitivity analysis of submerged arc welding process parameters[J]. Journal of Materials Processing Technology, 2008, 202(1): 500-507.

作者简介: 李培麟,男,1982 年出生,博士研究生. 主要从事焊接过程的有限元模拟方面的研究. 发表论文 5 篇. Email: windsome@163.com

通讯作者: 陆　皓,男,教授. Email: luhao@sjtu.edu.cn

Electronic Technology, Guilin 541004, China). p 73 - 76

Abstract: A novel image processing approach is proposed to reduce the mixed noise in surface mount technology soldering image based on wavelet packet transformed adaptive threshold. At first, by using wavelet packet transform, the approach not only decomposes the image into the low frequency part but also into the high frequency part of image in several scales. After analyzing the wavelet packet tree coefficients, they were processed with the Wiener filter, and kept the wavelet packet tree low frequency coefficients without change. Secondly, an improved wavelet adaptive threshold algorithm is proposed to denoise the mixed noise again. At last, the inverse wavelet packet transform is applied to reconstruct the image and median filter is used to smooth the image. The experimental results have illustrated that the approach can obtain a better result in soldering image denoising compared with the conventional methods and can retain the image edges very well.

Key words: surface mount technology solder joint; image denoising; wavelet packet transform; adaptive threshold

Compared study on properties of SnZn-based lead free solders LAI Zhongmin[1], ZHANG Liang[2], WANG Jianxin[1] (1. School of Materials Science & Engineering, Jiangsu University of Science and Technology, Zhenjiang 212003, China; 2. School of Mechanical & Electrical Engineering, Xuzhou Normal University, Xuzhou 221116, China). p 77 - 80

Abstract: The wettability, creep resistance and mechanical properties of four SnZn-based solders were compared. Base on the wetting-balance test, the wettability of SnZnAg/SnZnGa/SnZnAl is better than SnZn solders. The addition of alloying elements can improve the wettability of SnZn alloys. With the testing of nanoindentation creep behavior of SnZn solders, it is found that the creep resistance of SnZnAg solder is highest of all, the mechanism is Ag-Zn particles acting as barriers to the motion of dislocations. In addition, with the testing of mechanical properties, the results show that the mechanical and thermal-fatigue resistance properties can be enhanced with the addition of alloying elements, the mechanical properties of SnZnAg solder joints is 20% higher than that of SnZn solder joints, the function of Ga/Al is less than Ag. Furthermore, using diode laser soldering, the mechanical properties of SnZn solder joints can increase up to 116.7%.

Key words: lead-free solders; creep resistance properties; intermetallic compounds; diode laser soldering

Pitting corrosion resistance of micro-zones in welded joint of 2205 duplex stainless steel BAO Yefeng[1], HU Wangqin[1], JIANG Yongfeng[1], YANG Ke[1,2] (1. Institute of Mechanical and Electronic Engineering, Hohai University, Changzhou 213022, China; 2. Advanced Welding Technology of Provincial Key Laboratory, Jiangsu University of Science and Technology, Zhenjiang 212003, China). p 81 - 84

Abstract: The microstructures of welded joint of 2205 duplex stainless steel were studied by optical microscope. Cyclic voltammetry curves of base material, weld metal and HAZ were measured by a self-designed micro electrochemical system respectively. The results show that the microstructures of welded joint of 2205 duplex stainless steel are ferrite and austenite. The percentage of ferrite in weld metal is about 48%, which is equivalent with that in base material, while the average ferrite content in HAZ is more than a half. In the 3.5% NaCl solution, the weld metal shows the consistent pitting corrosion resistance with the base material, but its repassivation behavior is not as good as the base material. Among the three micro-zones of the welded joint, HAZ shows the poorest pitting corrosion resistance and repassivation behavior. The differences on pitting corrosion resistance of different micro-zones of welded joint are relevant to the phase ratio and the distribution of alloy elements in phases.

Key words: duplex stainless steel; microstructure; micro-electrochemical method; pitting corrosion

Impact toughness of simulated CGHAZ with high heat input for adding trace Zr oil tank steel LIANG Guoli[1,2,3], YANG Shanwu[1], WU Huibin[2], LIU Xueli[2] (1. Department of Material Physics and Chemistry, University of Science Technology of Beijing, Beijing 100083, China; 2. National Engineering Research Center for Advanced Rolling Technology, University of Science Technology of Beijing, Beijing 100083, China; 3. Department of Electro-Mechanical Engineering, Tangshan College, Tangshan 063000, China). p 85 - 88

Abstract: The effects of trace Zr element on impact toughness of coarse grain heat affected zone (CGHAZ) of 690 MPa grade oil tank steel was investingated with the high heat-input welding cycle using Gleeble3500. The results showed that trace Zr treated steel can significantly improve low temperature impact toughness of base metal, but it could seriously worsen the impact toughness of CGHAZ. The M-A component of trace Zr treated steel coarsed with the heat input increasing, the area percentage of M-A component decreased with the heat input increasing, which resulted in the steel toughness decreasing. The size of inclusions containing Zr are all micron level, and were precipitated in the solidification process, which have litte effect on strenghen and grain refinement, but has a very important influence on impact toughness. The oversize inclusions (1-3 μm) could result in the impact toughness decreasing.

Key words: oil tank steel adding trace Zr; high heat-input welding; CGHAZ; impact toughness

Sensitivity analysis and prediction of double ellipsoid heat source parameters LI Peilin, LU Hao (School of Material Science and Engineering, Shanghai Jiao Tong University, Shanghai 200240, China). p 89 - 91, 95

Abstract: When the arc force is strong, the double ellipsoid heat source model is the most widely used heat source model. The influence of the heat source parameters on the weld size was researched, and the sensitivity of the double ellipsoid heat source parameters was obtained for SAW. The multiple regression analysis was applied to research the relationship between the weld size and the heat source parameters. An empirical formula was put forward, and the heat source parameters corresponding to the weld width and penetration can be easily calculated by the empirical formula. The trial time is reduced and the simulation precision is increased.

Key words: submerged arc welding; double ellipsoid

heat source; sensitivity analysis; multiple regression analysis

Microstructure and performance of low matched welded joint by vibratory welding technology LIU Zhengjun, WANG Chuao, SU Yunhai (School of Material Science and Engineering, Shenyang University of Technology, Shenyang 110023, China). p 92 – 95

Abstract: In order to investigate the effect on the metallurgical structure and mechanical property of low matched high-tensile steel welded joint by vibratory welding technology, KPS-70 high-tensile steel welding wire was used as welding material in the experiment. It was welded by ($80\%Ar + 20\%CO_2$) gas shielded arc welding and was being vibrated mechanically in low frequency. The metallurgical structures and mechanical properties of welded joint with different vibratory parameters were analyzed using optical microscope, X-ray inflection, welded joint tensile test and deposited metal tensile test. The results show that the vibratory welding technology is able to improve strength and plasticity of weld metal. The size of grain of weld is refined. As the amplitude is too large, it will affect welding process parameters, which results in weld defects and deterioration of mechanical properties.

Key words: vibratory weld technology; high-tensile steel; low matched; mechanical property; metallurgical structure

Control system for anchor chain flash butt welder based on industrial PC SU Shijie[1], GAO Lili[2], WANG Xinyan[1] (1. Modern Manufacturing Technology Institute, Jiangsu University of Science and Technology, Zhenjiang 212003, China; 2. ZhongNan Anchor Chain Producing Co, Ltd, Zhoushan 211189, China). p 96 – 99

Abstract: Based on the industrial PC and multifunction data acquisition device, the control system for anchor chain flash butt welder was developed using Visual Studio Net 2003 and Measurement Studio, which could control the flash butt welding process in real time, manage the welding parameters, record the welding processes and etc. A dual closed-loop control that consists of industrial PC, high-precision displacement sensor, servo valve PID motion control module and servo valve was established to realize precise control of the electrodes. In order to avoid electromagnetic jamming, the methods including opto electric isolating, software and hardware filtering have been used. The results show that this system can precisely control the welder electrods motion, and the anchor chain welding quality is stable.

Key words: flash butt welding; anchor chain; servo control; control system

Variable parameters controlling method for auto-body multi-layered plates assembly MEI Dongsheng, ZHANG Zhongdian, LI Dongqing, WEI Yanhong (State Key Laboratory of Advanced Welding and Joining, Harbin Institute of Technology, Harbin 150001, China). p 100 – 103

Abstract: The same welding parameters was after adopted to generate welding nuggets of different vehicle type, thickness and layer number in auto-body assembly process, which caused many welding defects. Aiming at the above problem, the resistance spot welding monitoring system with micro control unit as its core was introduced, which could achieve the functions of data acquisition, data transmission and nugget number based welding automatic adjustment technology. Based on the analysis of process parameters, the welding technology adjustment accuracy evaluation algorithm was established, which could guarantee each welding spot obtained under appropriate welding technology. The test results indicate that the developed system is stable, accurate and appropriate for practical application.

Key words: auto-body assembly; resistance spot welding; variable parameters controlling; monitoring system

Research on two fuzzy neural networks to predict mechanical properties of welded joints ZHANG Yongzhi[1,2], DONG Junhui[1] (1. College of Materials Science and Engineering, Inner Mongolia University of Technology, Hohhot 010051, China; 2. Inner Mongolia Electric Power Engineering Research Institute, Hohhot 010050, China). p 104 – 107

Abstract: Due to high nonlinear, complex interaction of many factors in welding process, it was difficult to predict the mechanical properties of welded joints. In this paper the adaptive neuro-fuzzy inference system(ANFIS) and the fuzzy radial basis function network model had been established based on TC4 titanium alloy in TIG welding to predicate the mechanical properties of welded joints. The welding process parameters were regarded as the input and mechanical property as output parameters of prediction models. 27 sets of experimental data were used to train the model and another 6 sets of experimental data were used to make simulation. The results showed that two fuzzy neural network models have high prediction accuracy and can be used to predict the mechanical properties of welded joints. But in terms of the structure, training speed, stability, generalization ability and reflection of the true situations of network model, the fuzzy RBF neural network is better than adaptive neuron-fuzzy neural network.

Key words: adaptive neuro-fuzzy inference system; fuzzy RBF neural network; welding; mechanical properties; prediction

Status and development of electron beam surface alloying ZHANG Binggang, ZHAO Jian, FENG Jicai (State Key Laboratory of Advanced Welding and Joining, Harbin Institute of Technology, Harbin 150001, China). p 108 – 112

Abstract: This paper states the fundamental principle of electron beam surface alloying and the development of electron beam alloying equipment, introduces the application of high current pulsed electron beam as a new method in research, summarizes the development trend of research on electron beam surface alloying in recent years, and gives a sketch of main research achievements and progress at home and abroad. Controlling alloy layer quantitatively, thermo-mechanical coupling of electron beam, surface layer defect prevention and control, surface layer and advanced technology of electron beam welding will become the hot topics in future research. Electron beam surface alloying as a highly superior method of high energy density beams surface modification will play an important role.

Key words: electron beam welding; electron beam surface alloying; surface modification